Eur. Phys. J. C 49, 1023–1039 (2007)
DOI 10.1140/epjc/s10052-006-0177-3

THE EUROPEAN PHYSICAL JOURNAL C

Regular Article – Theoretical Physics

Non-standard Hamiltonian effects on neutrino oscillations

M. Blennow[1,a], T. Ohlsson[1,b], W. Winter[2,c]

[1] Department of Theoretical Physics, School of Engineering Sciences, Royal Institute of Technology (KTH) – AlbaNova University Center, Roslagstullsbacken 21, 10691 Stockholm, Sweden
[2] School of Natural Sciences, Institute for Advanced Study, Einstein Drive, Princeton, NJ 08540, USA

Received: 25 May 2006 / Revised version: 13 September 2006 /
Published online: 26 January 2007 –

Abstract. We investigate non-standard Hamiltonian effects on neutrino oscillations, which are effective additional contributions to the vacuum or matter Hamiltonian. Since these effects can enter in either the flavor or mass basis, we develop an understanding of the difference between these bases representing the underlying theoretical model. In particular, the simplest of these effects are classified as "pure" flavor or mass effects, where the appearance of such a "pure" effect can be quite plausible as a leading non-standard contribution from theoretical models. Compared to earlier studies investigating particular effects, we aim for a top–down classification of a possible "new physics" signature at future long-baseline neutrino oscillation precision experiments. We develop a general framework for such effects with two neutrino flavors and discuss the extension to three neutrino flavors, and we demonstrate the challenges for a neutrino factory to distinguish the theoretical origin of these effects with a numerical example as well. We find how the precision measurements of neutrino oscillation parameters can be altered by non-standard effects alone (not including non-standard interactions in the creation and detection processes) and that the non-standard effects on Hamiltonian level can be distinguished from other non-standard effects (such as neutrino decoherence and decay) if we consider the specific imprint of the effects on the energy spectra of several different oscillation channels at a neutrino factory.

1 Introduction

Neutrino physics has entered the era of precision measurements of the fundamental neutrino parameters such as the neutrino mass squared differences and leptonic mixing parameters, and neutrino oscillations are the most credible candidate for describing neutrino flavor transitions. Nevertheless, there might be other sub-leading mechanisms participating in the total description of neutrino flavor transitions. Thus, in this paper, we will investigate such mechanisms on a fundamental level, which will give rise to non-standard effects on the ordinary framework of neutrino oscillations.

In a previous paper [1], we have studied non-standard effects on probability level based on "damping signatures", which were phenomenologically introduced in the neutrino oscillation probabilities. However, in this paper, we will investigate so-called non-standard Hamiltonian effects, which are effects on the Hamiltonian level rather than on the probability level. Recently, three different main categories of non-standard Hamiltonian effects have been discussed in the literature. These categories are non-standard interactions (NSI), flavor-changing neutral currents (FCNC), and mass-varying neutrinos (MVN or MaVaNs). In addition, other effects which result in effective additions to the Hamiltonian have been studied, such as the effects of extra dimensions [2]. Below, we will briefly review the categories of the effects which can be studied using this framework.

In general, in many models, neutrino masses come together with NSI, which means that the evolution of neutrinos passing through matter is modified by non-standard potentials due to coherent forward-scattering of NSI processes $\nu_\alpha + f \to \nu_\beta + f$, where $\alpha, \beta = e, \mu, \tau$ and f is a fermion in matter.[1] The effective NSI potentials are given by $V_{\rm NSI} = \sqrt{2} G_{\rm F} N_d \tilde{\epsilon}_{\alpha\beta}$, where $G_{\rm F}$ is the Fermi coupling constant, N_d is the down quark number density, and the $\tilde{\epsilon}_{\alpha\beta}$ are small parameters describing the NSI [3]. See, e.g., [4] for a recent review. Furthermore, matter-enhanced neutrino oscillations in the presence of Z-induced FCNC have been studied in the literature [5–7]. See also, e.g., [8, 9] for some earlier contributions. Especially, NSI and FCNC have been investigated in several references for many different scenarios such as for so-

[a] e-mail: emb@kth.se
[b] e-mail: tommy@theophys.kth.se
[c] e-mail: winter@ias.edu

[1] Note that, in general, the production and detection vertices could also be modified. However, in this paper, we focus on the neutrino oscillation probabilities which, in the limit of ultra-relativistic neutrinos, decouple from the creation and detection processes.

lar [10–13],atmospheric [14–18], supernova [19], and other astrophysical neutrinos as well as for CP violation [20], the LSND experiment [21], beam experiments [22], and neutrino factories [23–28].

The idea of MVN was proposed by Fardon et al. in [29, 30]. This idea is based on the dark energy of the Universe being neutrinos which can act as a negative pressure fluid and may be the origin of cosmic acceleration. Furthermore, several continuation works on MVN have been performed in the context of scenarios for the Sun and the solar neutrino deficit [31, 32], but also in various other contexts [33–45]. In addition, it should be mentioned that neutrinos with variable masses have also been studied earlier than the idea of MVN [29, 46–49].

While earlier studies have discussed individual theoretical models and their effects on future neutrino oscillation experiments (bottom–up), our approach will be top–down. We start from general assumptions to investigate the properties of non-standard Hamiltonian effects, and later apply them to specific models and discuss how to identify individual effects. The goal of this approach is the classification of a possible "new physics" signature in future long-baseline neutrino oscillation experiments. Although it is very likely that such a signature will fit many different non-standard models, it has hardly been discussed in the literature how to distinguish (even qualitatively) different theoretical models which could all describe this effect, and what the methods for that identification could be. For this purpose, we make rather unspecific assumptions for the particular type of effect and rather assume that the theoretical model will predict a leading effect which can be considered to be of a "simple" form in a specific basis ("pure" effect), which can be either flavor (or mass) conserving or flavor (or mass) violating.

The paper is organized as follows. First, in Sect. 2, we define non-standard Hamiltonian effects as effective additional contributions to the vacuum Hamiltonian similar to matter effects. The definition is performed for n neutrino flavors. Next, in Sect. 3, we specialize our discussion to two neutrino flavors, where we derive the effective neutrino parameters as well as the resonance conditions in both flavor and mass bases including non-standard Hamiltonian effects. We also discuss experimental strategies to test and identify non-standard Hamiltonian effects at the example of $\nu_e \leftrightarrow \nu_\mu$ flavor transitions. Then, in Sect. 4, we study some aspects of the generalization to the three-flavor case, whereas in Sect. 5, we give a numerical example of how non-standard Hamiltonian effects can affect a realistic experimental setup and discuss how to tell non-standard Hamiltonian effects apart from damping effects. Finally, we summarize our results and present our conclusions in Sect. 6.

2 Parameterization of non-standard Hamiltonian effects

In the standard neutrino oscillation framework with n flavors, the Hamiltonian in vacuum is given by

$$H_0 = \frac{1}{2E} U \mathrm{diag}(m_1^2, m_2^2, \ldots, m_n^2) U^\dagger \,, \tag{1}$$

in the flavor basis, where E is the neutrino energy, U is the leptonic mixing matrix, and m_i is the mass of the ith neutrino mass eigenstate. Any Hermitian non-standard Hamiltonian effect will alter this vacuum Hamiltonian into an effective Hamiltonian:

$$H_{\mathrm{eff}} = H_0 + H' \,, \tag{2}$$

where H' is the effective addition to the vacuum Hamiltonian. We note that this reminds one of neutrino mixing and oscillations in matter [8] with H' given by a diagonal matrix with the effective matter potentials on the diagonal, i.e.,

$$H' = H_{\mathrm{mat}} = \mathrm{diag}(V, 0, \ldots, 0) - \frac{1}{\sqrt{2}} G_{\mathrm{F}} N_n \mathbf{1}_n \,, \tag{3}$$

where $V = \sqrt{2} G_{\mathrm{F}} N_e$ is the ordinary matter potential, G_{F} is the Fermi coupling constant, N_e is the electron number density (resulting from coherent forward-scattering of neutrinos), N_n is the nucleon number density, and $\mathbf{1}_n$ is the $n \times n$ unit matrix.[2] Just as the presence of matter affects the effective neutrino mixing parameters, the effective neutrino mixing parameters will be affected by any non-standard Hamiltonian effect. In the remainder of this text, we will treat the effective Hamiltonian

$$H_{\mathrm{eff}} = H_0 + H' + H_{\mathrm{mat}} \,, \tag{4}$$

i.e., we will treat the non-standard effects along with the matter effects. However, in Sect. 4, we treat only the part $H_0 + H'$ in order to obtain the parameters of the Hamiltonian to which the standard matter effects are then added. Since standard matter effects are generally taken into account, $H_0 + H'$ will be mistaken for the vacuum Hamiltonian H_0 if the non-standard effects are not considered.

Since any part of the effective Hamiltonian that is proportional to the $n \times n$ unit matrix only contributes with an overall phase to the final neutrino state, it will not affect the neutrino oscillation probabilities. This means that we may assume H' to be traceless and also that we may subtract $\mathrm{tr}(H)/n$ from the effective Hamiltonian to make it traceless. Any traceless Hermitian $n \times n$ matrix A may be written as

$$A = \sum_{i=1}^{N} c_i \lambda_i \,, \tag{5}$$

where the c_i are real numbers, the λ_i are the generators of the $SU(n)$ Lie algebra (i.e., A is an element of the Lie algebra), and $N = n^2 - 1$ is the number of generators. Hence, clearly, any non-standard Hamiltonian effect H' is parameterized by the $n^2 - 1$ numbers c_i. In summary, we choose

[2] If sterile neutrinos are present, then there is no interaction between the sterile neutrinos and the matter through which they propagate. Thus, the $\mathbf{1}_n$ term is replaced by a projection operator on the active neutrino states.

the coefficients of the generators of the $SU(n)$ Lie algebra to parameterize any non-standard Hamiltonian effect.

Furthermore, in any basis (e.g., flavor or mass basis), we may introduce $SU(n)$ generators λ_i such that $n(n-1)/2$ generators are off-diagonal with only two real non-zero entries, $n(n-1)/2$ generators are off-diagonal with only two imaginary non-zero entries, and $n-1$ generators are diagonal with real entries. For example, in the case of $n=2$, we have the Pauli matrices

$$\lambda_1 = \sigma_1 = \begin{pmatrix} 0 & 1 \\ 1 & 0 \end{pmatrix}, \quad \lambda_2 = \sigma_2 = \begin{pmatrix} 0 & -\mathrm{i} \\ \mathrm{i} & 0 \end{pmatrix}, \\ \lambda_3 = \sigma_3 = \begin{pmatrix} 1 & 0 \\ 0 & -1 \end{pmatrix}. \tag{6}$$

We will denote the set of generators which are of the form λ_i in the flavor basis by ρ_i and the set of generators which are of this form in the mass basis by τ_i. Obviously, in the flavor basis, we have the relations

$$\rho_i = \lambda_i \quad \text{and} \quad \tau_i = U\lambda_i U^\dagger, \tag{7}$$

where, in the case of two neutrino flavors,

$$U = \begin{pmatrix} \cos(\theta) & \sin(\theta) \\ -\sin(\theta) & \cos(\theta) \end{pmatrix}$$

is the two-flavor leptonic mixing matrix and θ is the corresponding mixing angle (when treating the three-flavor case, we will use the standard parameterization of the leptonic mixing with three mixing angles θ_{12}, θ_{23}, θ_{13}, and one CP violating phase δ_{CP}). This implies that ρ_i and τ_i would be equal if there were no mixing in the leptonic sector. Furthermore, it is obvious that the matrices ρ_i can be written as linear combinations of the matrices τ_i and vice versa. Therefore, there is, in principle, no difference between effects added in flavor or mass basis if one allows for the most general form of the non-standard contribution.

We now define any non-standard effect as a "pure" flavor or mass effect if the corresponding effective contribution to the Hamiltonian is given by

$$H' = c\rho_i \quad \text{or} \quad H' = c\tau_i \quad (i \text{ fixed}), \tag{8}$$

respectively, where $c \in \mathbb{R}$. This means that we restrict the "pure" effects to be of very specific types, where the actual forms are very simple in a given basis.[3] Given the possible theoretical origin, this approach is quite plausible if one assumes that the underlying theoretical model will produce one leading flavor (or mass) changing or conserving effect. Generally, the parameter c can depend on many different quantities, e.g., the matter density or the neutrino energy. In particular, the dependence on the neutrino energy ("spectral dependence") may allow for the unambiguous identification, or, in the case of mass-varying neutrinos, the matter density dependence may indicate this type of effect. However, any approach investigating such dependencies has to use specific models, and the actual representation by Nature may easily be overseen. Therefore, we do not require this information in this study and rather investigate the generic impact of effects in the flavor or mass basis. In addition, we note that the matter density or energy dependence of the non-standard effects should be very weak for a given terrestrial experiment with a specific matter density profile. Only for effects motivated by MVN, i.e., mass effects, we will use the same energy dependence as for the masses themselves for numerical simulations. In general, if a large span of energies is available, one should of course also try to distinguish different specific models through their different energy dependencies.

This choice of pure effects implies that only one of the generators of the Lie algebra is present, since a general linear combination, such as (5), can always be interpreted in both bases. Thus, we define a flavor or mass conserving (violating) effect as any effect where the effective contribution to the Hamiltonian is diagonal (off-diagonal) in the corresponding basis.[4] We note that a pure flavor (mass) violating effect corresponds to some interaction between two flavor (mass) eigenstates. For example, the $SU(2)$ generators ρ_1 and ρ_2 correspond to flavor-violating (or changing) effects, whereas ρ_3 corresponds to flavor-conserving effects. In summary, if we detect an arbitrary non-standard effect, it is the simple form in flavor or mass basis which makes it a flavor or mass effect by our definition. This approach can be justified by the fact that the simplest models for non-standard effects from the underlying theory correspond to specific patterns for the effective addition to the Hamiltonian. Therefore, our definition of a "pure" effect is a conceptually new one, and it refers to a class of effects which can be interpreted in different ways. However, since simplicity is a basic concept in physics, this concept allows the choice of the most "natural" non-standard effects for further testing.

The case of non-standard Hamiltonian effects on three-flavor neutrino oscillations, i.e., the case of $n=3$, is quite similar to the one described above for the two-flavor case. Instead of the Pauli matrices, which are a basis of the $SU(2)$ Lie algebra, we now have to use the eight Gell-Mann matrices, which span the $SU(3)$ Lie algebra. Out of the Gell-Mann matrices, three are off-diagonal with two real entries, three are off-diagonal with two imaginary entries, and two are diagonal with real entries. Even though the principle of the three-flavor case is the same as that of the two-flavor case, it introduces many more parameters (more leptonic mixing angles, the complex phase in the leptonic mixing matrix, the extra mass squared difference, and the

[3] Because of our choice to use the Pauli matrices, a "pure" effect corresponds to the interaction of two flavor or mass eigenstates. This is also the reason for choosing to work with the Pauli matrices. In addition, it is also interesting to keep the real and complex parts of the off-diagonal entries separate (i.e., not working with the complex matrix elements directly, but rather a set of real parameters) in order to investigate the possibilities of probing CP violation effects.

[4] Strictly speaking, our definition distinguishes (in two flavors) off-diagonal additions proportional to λ_1 (real) or λ_2 (complex).

extra degrees of freedom for the non-standard effects), and therefore, turns out to be much more cumbersome to handle than the two-flavor case. In the following, we will therefore start by treating the two-flavor case in some detail and then continue by studying the similarities and differences when approaching the full three-flavor case.

As far as the classification of current models in our notation is concerned, NSI and FCNC will be flavor effects, whereas MVN will produce mass effects. In general, NSI can be of two types: flavor changing (FC) and non-universal (NU) [4]. The off-diagonal elements of the effective NSI potential $\epsilon_{\alpha\beta}$, where $\alpha \neq \beta$, correspond to FC, whereas the differences in the diagonal elements $\epsilon_{\alpha\alpha}$ correspond to NU. In addition, FCNC are flavor-violating effects and MVN can be mass conserving. In principle, for our purposes, there is no difference between FC NSI and FCNC.

3 Non-standard Hamiltonian effects in the two-flavor limit

In this section, we study the general implications of non-standard Hamiltonian effects in the two-flavor limit. We discuss the effective parameter mapping including non-standard effects, and then we apply it to a two-flavor limit as an example.

3.1 Parameter mapping in two flavors

In Appendix A, we describe the general formalism of the two-flavor scenario, which can be used to obtain the results in this section. First, we discuss effects given in the flavor basis, which are effects expanded in ρ_i [cf. (7)]. In this case, flavor-conserving effects will be contributions to the total Hamiltonian on the form $H' = F_3\rho_3$, where $F_3 \in \mathbb{R}$, whereas flavor-violating effects will be contributions of the form $H' = F_1\rho_1 + F_2\rho_2$, where $F_i \in \mathbb{R}$. In the flavor basis, the new effective parameters are given by

$$\Delta\tilde{m}^2 = \Delta m^2 \xi \,, \tag{9}$$

$$\sin^2(2\tilde{\theta}) = \frac{\left[\frac{4EF_1}{\Delta m^2} + \sin(2\theta)\right]^2 + \left(\frac{4EF_2}{\Delta m^2}\right)^2}{\xi^2} \,, \tag{10}$$

where

$$\xi = \left\{ \left[\frac{4EF_1}{\Delta m^2} + \sin(2\theta)\right]^2 + \left(\frac{4EF_2}{\Delta m^2}\right)^2 + \left[\frac{2VE}{\Delta m^2} + \frac{4EF_3}{\Delta m^2} - \cos(2\theta)\right]^2 \right\}^{1/2} \tag{11}$$

is the normalized length of the Hamiltonian vector (see Appendix A), $\Delta\tilde{m}^2$ is the effective mass squared difference in the flavor basis, and $\tilde{\theta}$ is the effective mixing angle in the flavor basis.[5] In addition, the resonance condition is found to be

$$\frac{2VE}{\Delta m^2} + \frac{4EF_3}{\Delta m^2} = \cos(2\theta) \,, \tag{12}$$

which is clearly nothing but a somewhat modified version of the Mikheyev–Smirnov–Wolfenstein (MSW) resonance condition [8, 50, 51]. From the resonance condition in (12), it is easy to observe that the resonance is present for some energy E if and only if

$$\mathrm{sgn}(\Delta m^2)\mathrm{sgn}(V)\mathrm{sgn}(1 + 2F_3/V) = \mathrm{sgn}[\cos(2\theta)] \,, \tag{13}$$

where $\mathrm{sgn}(\Delta m^2)$ is dependent on the mass hierarchy, $\mathrm{sgn}(V)$ is dependent on if we are studying neutrinos or antineutrinos, and $\mathrm{sgn}(1 + 2F_3/V)$ is dependent on the ratio between F_3 and the matter potential V [$\mathrm{sgn}(1 + 2F_3/V)$ being equal to -1 if and only if F_3 has a magnitude larger than $|V/2|$ and is of opposite sign to V]. Note that if there are flavor-violating contributions added to the Hamiltonian, then these do not change the resonance condition. The sign of $\cos(2\theta)$ can be made positive by reordering the mass eigenstates in the case of two neutrino flavors. However, we keep this term as it is, since this is not possible in the case of three neutrino flavors. This resonance condition can be easily understood, since the effective contribution to the Hamiltonian from any flavor-violating effect will be parallel to the $H_3 = 0$ plane, i.e., these contributions are off-diagonal.

If we choose to describe the non-standard addition to the Hamiltonian in the mass eigenstate basis, then we find that the mixing parameters are given by

$$\Delta\tilde{m}^2 = \Delta m^2 \xi \,, \tag{14}$$

$$\sin^2(2\tilde{\theta}) = \frac{\left[\frac{4EM_1}{\Delta m^2}\cos(2\theta) + \left(1 - \frac{4EM_3}{\Delta m^2}\right)\sin(2\theta)\right]^2 + \left(\frac{4EM_2}{\Delta m^2}\right)^2}{\xi^2} \,, \tag{15}$$

where

$$\xi = \left\{ \left[\frac{2VE}{\Delta m^2}\sin(2\theta) + \frac{4EM_1}{\Delta m^2}\right]^2 + \left(\frac{4EM_2}{\Delta m^2}\right)^2 + \left[\frac{2VE}{\Delta m^2}\cos(2\theta) + \frac{4EM_3}{\Delta m^2} - 1\right]^2 \right\}^{1/2} \,, \tag{16}$$

and the resonance condition becomes

$$\frac{2VE}{\Delta m^2} + \frac{4EM_1}{\Delta m^2}\sin(2\theta) + \frac{4EM_3}{\Delta m^2}\cos(2\theta) = \cos(2\theta) \,. \tag{17}$$

Note that both mass conserving effects and mass violating effects enter into the resonance condition, whereas only the flavor-conserving effects entered in the corresponding expression in the flavor basis cf., (12). This is due to the fact that the changes of the Hamiltonian vector from such ef-

[5] Note that F_2 may also change the effective Majorana phase.

fects are not parallel to the $H_3 = 0$ plane (in flavor basis, see Appendix A), i.e., both of these effects affect the diagonal terms of the total Hamiltonian. However, M_2 does not enter into the resonance condition, since $\sigma_2 = \tau_2$, i.e., the change of the Hamiltonian is off-diagonal also in the flavor basis.

3.2 Interpretation of experiments in the two-flavor limit

Since a general analytic discussion of three-flavor neutrino oscillations including non-standard Hamiltonian effects would be very complicated, we focus on two neutrino flavors in this section. This approach can be justified if one assumes that the other contributions are exactly known or the two-flavor probabilities dominate. Of course, for short-term applications, small non-standard effects might be confused with other small effects such as $\sin^2(2\theta_{13})$ effects [27]. Thus, a comprehensive quantitative discussion would be very complicated at present.

In three-flavor neutrino oscillations, we can construct several interesting two-flavor limits of the probabilities $P_{\alpha\beta}$ including non-standard effects related to two-flavor neutrino oscillations (see, e.g., [52]):

$$P_{ee} \underset{\Delta m^2_{21}\to 0}{\longrightarrow} 1 - \sin^2(2\tilde{\theta}_{13}) \sin^2\left(\frac{\Delta\tilde{m}^2_{31} L}{4E}\right), \tag{18}$$

$$P_{ee} \underset{\theta_{13}\to 0}{\longrightarrow} 1 - \sin^2(2\tilde{\theta}_{12}) \sin^2\left(\frac{\Delta\tilde{m}^2_{21} L}{4E}\right), \tag{19}$$

$$P_{\mu e} \underset{\Delta m^2_{21}\to 0}{\longrightarrow} \sin^2(2\tilde{\theta}_{13}) \sin^2\left(\frac{\Delta\tilde{m}^2_{31} L}{4E}\right) \sin^2(\theta_{23}), \tag{20}$$

$$P_{\mu\mu} \underset{\Delta m^2_{21}\to 0,\, \theta_{13}\to 0}{\longrightarrow} 1 - \sin^2(2\tilde{\theta}_{23}) \sin^2\left(\frac{\Delta\tilde{m}^2_{31} L}{4E}\right). \tag{21}$$

Note that all of these probabilities also contain the standard matter effects except for $P_{\mu\mu}$. In general, the $SU(3)$ generators (the Gell-Mann matrices) will give the degrees of freedom for non-standard Hamiltonian effects with three flavors. However, when studying the effective two-flavor neutrino oscillations, we only use the Gell-Mann matrices which are the equivalents of the Pauli matrices in the two-flavor sector that is studied. In addition, one can create two-flavor limits for oscillations into sterile neutrinos, such as in [2]. In the following, we will focus on small mixing and the case of (20) for illustration. We discuss the large mixing case in Appendix B. In addition, see Appendix C for subtleties with the definitions of the effective two-flavor scenarios.

For small mixing, such as for (20), we show in Fig. 1 the neutrino oscillation appearance probability $P_{\alpha\beta}$ for two flavors with small mixing, where the effects of the F_i are parameterized relative to the matter effects (i.e., "1" on the vertical axis corresponds to an effect with $F_i = V$ and "0" to no non-standard effects). In this figure, many of the following analytic observations are visualized. The resonance condition in (12) can always be fulfilled for the matter resonance ($F_3 = 0$) by an appropriate choice of energy, baseline, neutrinos or antineutrinos, and oscillation channel. Obviously, we can read off from (10) that at the resonance $\sin^2(2\tilde{\theta}) \to 1$, where the matter resonance condition can be influenced by F_3 according to (12). Therefore, the magnitude of $\sin^2(2\tilde{\theta})$ at the resonance (but not necessarily $P_{\alpha\beta}$) is independent of F_1, F_2, and F_3 by definition. However, F_3 can shift the position of the resonance (such as in energy space). If we choose an energy far above the resonance energy and $F_i/V \ll 1$ ($i = 1, 2, 3$), then we have

$$\sin^2(2\tilde{\theta}) \to \frac{\left[\frac{4EF_1}{\Delta m^2} + \sin(2\theta)\right]^2 + \left(\frac{4EF_2}{\Delta m^2}\right)^2}{\left[\frac{2VE}{\Delta m^2} + \frac{4EF_3}{\Delta m^2} - 1\right]^2}. \tag{22}$$

This means that F_1 and F_2 can, for large enough energies, enhance a flavor transition, i.e., they increase the oscillation amplitude. In principle, one could distin-

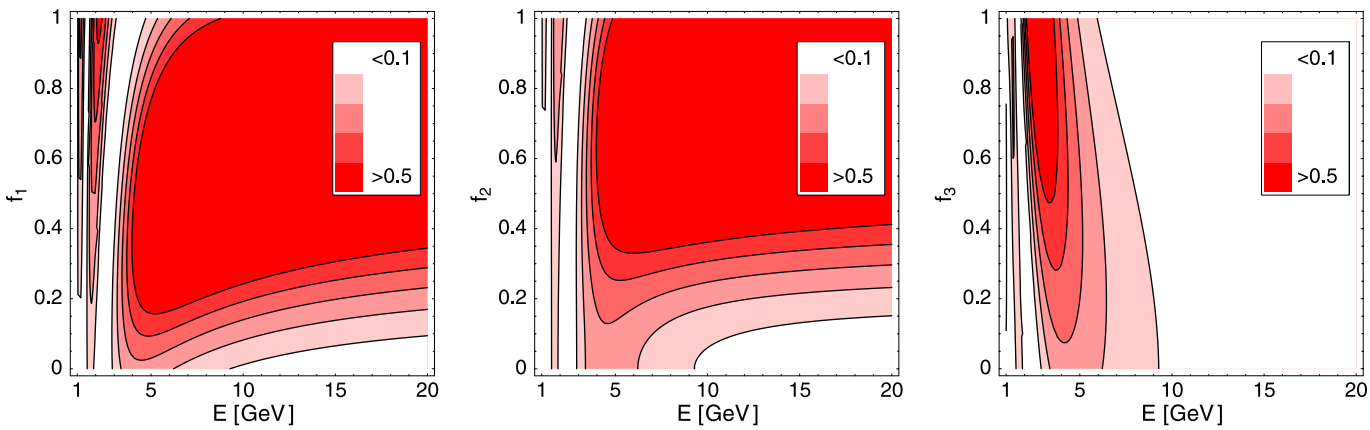

Fig. 1. The two-flavor appearance probability $P_{\alpha\beta}$ as a function of energy and the flavor-conserving/violating fraction $f_i \equiv F_i/V$ (normalized relative to matter effects). For the values of the neutrino parameters, we have used $\theta = 0.16 \simeq 9.2^\circ$, $\Delta m^2 = 0.0025\ \mathrm{eV}^2$, $L = 3000$ km, $\rho = 3.5\ \mathrm{g/cm}^3$, neutrinos only, $\Delta m^2 > 0$, and $f_i > 0$

guish F_1 from F_2 by a measurement at two different energies, because the mixed term from the square in the numerator of (22) has a linear (instead of quadratic) energy dependence. In practice, such a discrimination should be very hard. In addition, the quantity F_3 can play the same role as the matter potential V, i.e., it can change the flavor transition for large energies. It is also obvious from (10) and (11) that F_3 can affect the matter resonance energy and that it is directly correlated with the matter potential V, i.e., one cannot establish effects more precisely than the matter density uncertainty.

In Sect. 3.1, we have also discussed mass effects, such as coming from MVN. Since a pure M_1 or M_3 effect translates into a combination of F_1 and F_3 cf., (A.6), we expect to find a mixture of F_1 and F_3 effects, i.e., both F_1 and F_3 effects have to be present. Thus, if we assume that there is only one dominating "pure" non-standard contribution (F_1, F_2, F_3, M_1, M_2, or M_3), then this simultaneous presence points toward a mass effect. Clearly, an M_2 effect, on the other hand, cannot be distinguished from an F_2 effect; cf. (A.6). A different property of M_3, which is not so obvious from Sect. 3.1, but very obvious already from (1), (2), and (7) is this: since M_3 is diagonal in the mass basis, it corresponds to an energy dependent shift of the vacuum mass squared difference. As a consequence, in vacuum, the effective mixing angle is not modified by M_3; cf. (15). Thus, the oscillation amplitudes are not modified by M_3, but the oscillation pattern shifts (contrary to F_3 effects, where also the amplitude changes). In this case, the resonance condition becomes meaningless and the amplitude becomes $\sin^2(2\tilde{\theta}) = \sin^2(2\theta)$. Note that a direct test using one experiment only makes it hard to identify mass effects uniquely if they are introduced with the same energy dependence as the vacuum masses (because they can be rotated away by a different set of neutrino oscillation parameters). Thus, other methods might be preferable, such as modified MSW transitions in the Sun [31, 32] or reactor experiments comparing air and matter oscillations [53]).

Another class of effects has been discussed by Blennow et al. in [1]. In this study, so-called "damping effects" could describe modifications on the probability level instead of the Hamiltonian level (such as neutrino decay, absorption, wave packet decoherence, oscillations into sterile neutrinos, quantum decoherence, averaging, etc.). It is obvious from (3) in [1] that these damping effects do not alter the oscillation frequency, while we can read off from (9) and (11) that it is a general feature of non-standard Hamiltonian effects that the oscillation frequency is changed. However, for damping effects, the oscillation amplitude can be damped either by a damping of the overall probability ("decay-like damping") or by the oscillating terms only ("decoherence-like damping"). In the first case, the total probability of finding a neutrino in any neutrino state is damped for all energies, whereas in the second case it is constantly equal to one while the individual neutrino oscillation probabilities are damped in the oscillation maxima and enhanced in the oscillation minima. Since all (small) effects one could imagine in quantum field theory, involving the modification of fundamental interactions or propagations, can be described by either a coherent or incoherent addition of amplitudes, one can expect that the two classes of Hamiltonian and probability (damping) effects can cover all possible effects. However, in practice, potential energy, environment, and explicit time dependencies (such as from a matter potential) can make life more complicated.

4 Three-flavor effects

As was stated in the Sect. 2, the general three-flavor case is quite complicated. However, if we assume that the non-standard effects are small, then we can use perturbation theory to derive expressions for the change in the neutrino oscillation parameters. For example, the elements of the effective mixing matrix are given by

$$\tilde{U}_{\alpha i} = \langle \nu_\alpha | \tilde{\nu}_i \rangle \ , \tag{23}$$

where $|\tilde{\nu}_i\rangle$ is the eigenstate of the full Hamiltonian. To first order in perturbation theory, we have

$$|\tilde{\nu}_i\rangle = |\nu_i\rangle + \sum_{j \neq i} \frac{\langle \nu_j | H' | \nu_i \rangle}{E_i - E_j} |\nu_j\rangle \simeq |\nu_i\rangle + 2E \sum_{j \neq i} \frac{H'_{ji}}{\Delta m^2_{ji}} |\nu_j\rangle \ , \tag{24}$$

and thus we find

$$\tilde{U}_{\alpha i} \simeq U_{\alpha i} + 2E \sum_{j \neq i} \frac{H'_{ji}}{\Delta m^2_{ji}} U_{\alpha j} \ , \tag{25}$$

or, in terms of the non-standard addition given in the flavor basis,

$$\tilde{U}_{\alpha i} \simeq U_{\alpha i} + 2E \sum_{j \neq i} \sum_{\beta,\gamma} \frac{U_{\beta j} U^*_{\gamma i} H'_{\beta\gamma}}{\Delta m^2_{ji}} U_{\alpha j} \ . \tag{26}$$

We note that this approach is valid only if $|2EH'_{ij}/\Delta m^2_{ji}| \ll 1$. If this is not valid, then we have to use degenerate perturbation theory in order to obtain valid results.

It was discussed in [26, 27], that if θ_{13} is small enough, then possible NSI in the creation, propagation, and detection processes may mimic the effects of a larger θ_{13} (this can also be the case for other effects which are not usually treated along with neutrino oscillations, such as damping effects [1]). Here, we consider only the propagation effects separately and consider how this alone could affect the determination of θ_{13}. The reason for doing so is that, while NSI can also affect the creation and detection processes, other non-standard effects, e.g., MVN, may not. With the perturbation theory approach described above, this becomes very transparent and is probably one of the most interesting applications of non-standard effects. In any experimental setup, the value of the mixing angle θ_{13} is determined by the modulus of the element U_{e3} of the neutrino mixing matrix U. If we include non-standard effects, then

the effective counterpart of this element is given by

$$\tilde{U}_{e3} \simeq U_{e3} + \frac{2E}{\Delta m^2_{31}} \left(1 + \alpha s^2_{12}\right) \left(s_{23} H'_{e\mu} + c_{23} H'_{e\tau}\right) + \alpha \frac{2E}{\Delta m^2_{31}} s_{12} c_{12} \times \left[c^2_{23} H'_{\mu\tau} - s^2_{23} H'_{\tau\mu} + \frac{1}{2} \sin(2\theta_{23}) \left(H'_{\mu\mu} - H'_{\tau\tau}\right)\right], \quad (27)$$

where we have made a series expansion to first order in $\alpha = \Delta m^2_{21}/\Delta m^2_{31} \simeq 0.03$ and disregarded terms of second order in both H' and θ_{13}.

If U_{e3} is smaller than or of equal size to the other terms in this expression, then the θ_{13} determined by an experiment will not be the actual θ_{13} unless the non-standard effects are taken into account. It is worth to notice that if $\theta_{23} = 45°$, then $c_{23} = s_{23}$ and only the imaginary part of $H'_{\mu\tau} = (H'_{\tau\mu})^*$ will enter into the expression for $\tilde{U}_{e3}$, indicating that if the leading term is the one containing $H'_{\mu\tau}$, then the effective CP violating phase will be $\pm 90°$. Another interesting observation is that even if there are no non-standard effects, there is a term proportional to $\Delta V \equiv H'_{\mu\mu} - H'_{\tau\tau}$ in this expression. Because of the different matter potentials for ν_μ and ν_τ due to loop level effects, this quantity will be of the order $\Delta V \simeq 10^{-5} V$.

In Fig. 2, we plot the possible range of $|\tilde{U}_{e3}|$ as a function of $\epsilon_{\max} VE$, where $H'_{\alpha\beta} = \epsilon_{\alpha\beta} V$, V is the matter potential, and $|\epsilon_{\alpha\beta}| < \epsilon_{\max}$. For comparison, a neutrino factory with a neutrino energy of $E = 50$ GeV and a matter density of $3\,\mathrm{g/cm^3}$ will have $VE \simeq 6 \times 10^{-15}\,\mathrm{MeV}^2$ and the position at which we need to consider the possible range of $|\tilde{U}_{e3}|$ then depends on the bounds on the non-standard parameters $\epsilon_{\alpha\beta}$. In general, the bounds for $\epsilon_{\alpha\beta}$ depend on the type of non-standard effect and the types of interactions that are considered. In the case of NSI, it is common to write the non-standard interaction parameters as

$$\epsilon_{\alpha\beta} = \sum_f \epsilon^f_{\alpha\beta} \frac{N_f}{N_e}\,, \quad (28)$$

where we sum over different types of fermions, $\epsilon^f_{\alpha\beta}$ depends on the non-standard interaction with the fermion f, and N_f is the number density of the fermion f. In addition, $\epsilon^f_{\alpha\beta}$ is often split into $\epsilon^f_{\alpha\beta} = \epsilon^{fL}_{\alpha\beta} + \epsilon^{fR}_{\alpha\beta}$, where L and R denote the projectors used in the fermion factor of the effective non-standard Lagrangian density, i.e.,

$$\mathcal{L}_{\mathrm{eff}} = -2\sqrt{2} G_{\mathrm{F}} \sum_f \sum_{P=L,R} \epsilon^{fP}_{\alpha\beta} (\bar{\nu}_\alpha \gamma_\rho L \nu_\beta)(\bar{f} \gamma^\rho P f)\,. \quad (29)$$

Recent bounds for $\epsilon^{fP}_{\alpha\beta}$ can be found in [54] for electron neutrino interactions with electrons (i.e., $\epsilon^{eP}_{e\beta}$) and in [55] for interactions with first generation standard model fermions. As an example, the bounds from [54] for the $\epsilon_{e\tau}$ (which is considered in Fig. 2) are

$$-0.90 < \epsilon^{eL}_{e\tau} < 0.88 \quad \text{and} \quad -0.45 < \epsilon^{eR}_{e\tau} < 0.44\,, \quad (30)$$

respectively. This means that the bounds, especially in this sector, are weak, which we will use in the next section.

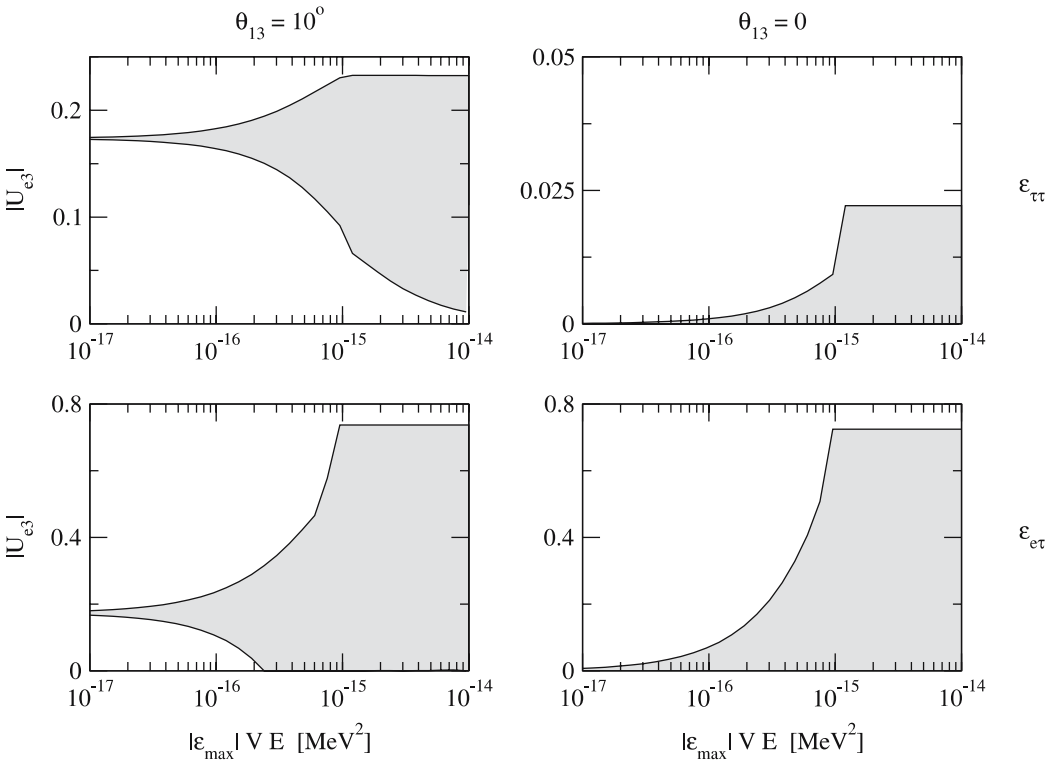

Fig. 2. The range of possible $|\tilde{U}_{e3}|$ as a function of $\epsilon_{\max} VE$. The plots are arranged so that the *left panels* correspond to $\theta_{13} = 10°$ and the *right panels* to $\theta_{13} = 0$, while the *lower panels* correspond to a non-standard effect with $\epsilon_{e\tau} \neq 0$ and the *upper panels* to a non-standard effect with $\epsilon_{\tau\tau} \neq 0$. The qualitative behavior for other values of θ_{13} is similar to the behavior for $\theta = 10°$. (Note the different scales on the vertical axes)

From Fig. 2, we can deduce that the off-diagonal $\epsilon_{e\tau}$ terms have a larger potential of altering the value of $|\tilde{U}_{e3}|$ than the diagonal $\epsilon_{\tau\tau}$ terms; the maximal value can even exceed $1/\sqrt{2}$, corresponding to $\tilde{\theta}_{13} = 45^\circ$. In addition, it is possible to suppress the effective θ_{13} to zero if introducing non-standard effects. It follows that a relatively large θ_{13} signal, bounded only by the size of the non-standard effects, can be induced or that a large θ_{13} signal can be suppressed by non-standard effects. Note that the effects quickly disappear at low energies, e.g., in reactor experiments. In order to tell a genuine θ_{13} signal apart from a signal induced by non-standard interactions, it is necessary to study the actual distortion of the energy spectrum induced by the neutrino oscillations.

5 A numerical example: neutrino factory for large $\sin^2(2\theta_{13})$

This section is not supposed to be a complete study of non-standard Hamiltonian effects, but to demonstrate some of the properties qualitatively discussed in the last sections in a complete numerical simulation of a possible future experiment using the exact three-flavor probabilities. Therefore, we have to make a number of assumptions. We use a modified version of the GLoBES software [56] to include non-standard effects. As a future high-precision instrument, we choose the neutrino factory experiment setup from [57, 58] with $L = 3000\,\mathrm{km}$, a 50 kt magnetized iron calorimeter detector, 1.06×10^{21} useful muon decays per year, and four years of running time in each polarity.[6] This experiment uses muon neutrino disappearance and electron to muon neutrino appearance as oscillation channels for both neutrinos and antineutrinos (in the muon and antimuon operation modes combined). For the neutrino oscillation parameters, we use $\sin^2 2\theta_{12} = 0.83$, $\sin^2 2\theta_{23} = 1$, $\Delta m^2_{21} = 8.2 \times 10^{-5}\,\mathrm{eV}^2$, and $\Delta m^2_{31} = 2.5 \times 10^{-3}\,\mathrm{eV}^2$ [59–62], as well as making the assumption of a 5% external measurement for Δm^2_{21} and θ_{12} [60] and including matter density uncertainties of the order of 5% [63, 64]. In order to test precision measurements of the non-standard effects, we use $\sin^2(2\theta_{13}) = 0.1$, which is close to the CHOOZ upper bound[7] [67]; also, we assume a normal mass hierarchy and $\delta_{\mathrm{CP}} = 0$. For simplicity, we do not take the $\mathrm{sgn}(\Delta m^2_{31})$-degeneracy [68] into account, but we include the intrinsic $(\theta_{13}, \delta_{\mathrm{CP}})$-degeneracy [69], whereas the octant degeneracy does not appear for maximal mixing [70]. Note that we do *not* include external bounds on the non-standard physics and $\sin^2(2\theta_{13})$, which, for instance, means that we allow for "fake" solutions of $\sin^2(2\theta_{13})$ above the CHOOZ bound. This assumption is plausible, since, depending on the effect, the CHOOZ bound may have been affected by the non-standard effect as well.

5.1 Test model

Since we choose $\sin^2(2\theta_{13})$ to be large, let us first of all focus on the appearance channel of ν_e oscillating into ν_μ (or $\bar{\nu}_e$ oscillating into $\bar{\nu}_\mu$). Expanding in small $\sin^2(2\theta_{13})$ and $\alpha \equiv \Delta m^2_{21}/\Delta m^2_{31}$, we have for $\alpha \to 0$ (which should be a good approximation for $\sin^2(2\theta_{13}) \gg \alpha^2 \simeq 0.001$) [71–73]

$$P_{e\mu} \sim \sin^2 2\theta_{13} \sin^2\theta_{23} \frac{\sin^2[(1-\hat{A})\Delta]}{(1-\hat{A})^2}\,, \tag{31}$$

where $\Delta \equiv \Delta m^2_{31} L/(4E)$ and $\hat{A} \equiv \pm 2\sqrt{2} G_{\mathrm{F}} n_e E/\Delta m^2_{31}$. Similarly, $P_{e\tau}$ is described by this equation with $\sin^2\theta_{23}$ replaced by $\cos^2\theta_{23}$. This means that we may be effectively dealing with the two-flavor limits described in Sect. 3, depending on the degree that the non-standard effects are different for the μ and τ flavors (cf. Appendix C).

Using the parameterization in (5) and (6) applied to the 1–3-sector, we therefore adopt the following Hamiltonian:

$$H_{\mathrm{eff}} = \frac{1}{2E} U \begin{pmatrix} \tilde{M}_3 & 0 & \tilde{M}_1 - \mathrm{i}\tilde{M}_2 \\ 0 & \Delta m^2_{21} & 0 \\ \tilde{M}_1 + \mathrm{i}\tilde{M}_2 & 0 & \Delta m^2_{31} - \tilde{M}_3 \end{pmatrix} U^\dagger + \begin{pmatrix} V + F_3 & 0 & F_1 - \mathrm{i}F_2 \\ 0 & 0 & 0 \\ F_1 + \mathrm{i}F_2 & 0 & -F_3 \end{pmatrix}. \tag{32}$$

In this model, M_1 and M_2 correspond to the CP conserving and CP violating parts of a mass-changing effect, whereas M_3 is a mass conserving effect. In addition, F_1 and F_2 are the CP conserving and CP violating parts of a flavor-changing effect, whereas F_3 is a flavor-conserving effect. As motivated before, it is plausible to assume that one of these non-standard effects may be dominating the other ones, because many models predict such a dominating component and the experimental constraints on some quantities are rather strong. In addition, (32) implies that the effects are mainly present in the 1–3-sector, which can be motivated by rather weak experimental bounds on the ν_τ-sector. For example, the bounds on the matrix element $H'_{e\tau}$ are rather weak in the case of NSI, making it viable that this term is dominating the NSI Hamiltonian. In this case, we obtain

$$H' = V \begin{pmatrix} 0 & 0 & \epsilon_{e\tau} \\ 0 & 0 & 0 \\ \epsilon^*_{e\tau} & 0 & 0 \end{pmatrix} \Leftrightarrow F_1 = V\mathrm{Re}(\epsilon_{e\tau}),\quad F_2 = V\mathrm{Im}(\epsilon_{e\tau})\,. \tag{33}$$

[6] Compared to [57], we use a 2.5% systematic normalization error for all channels as in [58].

[7] In general, a large $\sin^2(2\theta_{13})$ will imply a large signal in the appearance channel. However, non-zero effective $\sin^2(2\theta_{13})$ could arise even if $\sin^2(2\theta_{13}) = 0$; cf.Fig. 2. For effects which are diagonal in the flavor basis, a large $\sin^2(2\theta_{13})$ would be preferred in order to make an observation of the non-standard effect. We have used a large $\sin^2(2\theta_{13})$ as an example, since one may argue that the finding of new effects at present experiments (such as MINOS) may lead to a good reason for constructing a neutrino factory. One should also observe that, in principle, it would be possible to find non-standard effects at, e.g., MINOS [65, 66]. However, the precision of a neutrino factory would be more sensitive to small effects, and, thus, be more useful for distinguishing between effects.

Thus, we have a flavor-violating effect with F_1 representing the CP conserving part of the NSI, and F_2 representing the CP violating part of the NSI. The form of the mass effects has been chosen to match the expected energy dependence of MVN in order to discuss effects with realistic spectral (energy) dependencies.

Note that the parameterization in (32) does not exactly correspond to the two-flavor limit even for $\alpha \to 0$, since there are some non-trivial mixing effects in the 2–3-sector as described in Appendix C. This parameterization is also obviously not the whole story in the three-flavor scenario. For instance, we assume the same sign for effects on neutrinos and antineutrinos, which may, depending on the model, not apply in general. However, we will demonstrate some of the characteristics from Sect. 3.2 with this approach. In addition, note that we have now adopted a specific energy dependence of the flavor and mass effects, where the definition of the energy dependence in the $\tilde{M}$ is slightly different from the one in the M in Sect. 2; i.e., $M \equiv \tilde{M}/(2E)$. In this case, the mass effects could be coming from MVN changing the mass eigenstates, whereas the flavor effects correspond to some NSI approximately constant in the considered energy range. We will quantify the size of the F_i and $\tilde{M}_i$ in terms of the normalized quantities $f_i \equiv F_i/V$ (for $\rho = 3.5\,\mathrm{g/cm^3}$) and $\mu_i \equiv \tilde{M}_i/\Delta m^2_{31}$ (for $\Delta m^2_{31} = 2.5 \times 10^{-3}\,\mathrm{eV}^2$). This quantification makes sense, since it is obvious from (32) that the effect of these quantities will have to be compared with the order of V and Δm^2_{31}, respectively. Note that $f_1 - \mathrm{i} f_2 = \epsilon^e_{e\tau}$ from Sect. 4, which means that it will be interesting to compare the precision of f_1 and f_2 to the current bounds for $\epsilon_{e\tau}$. Furthermore, note that the mass effects can be simply rotated away by a different choice of the mixing matrix and the mass squared differences, because of the same energy dependence in this example. However, since we assume the solar parameters to be measured externally, we will observe that constraints to the $\tilde{M}_i$ can be derived. Such an external measurement with an environment dependence similar to the neutrino factory comes from KamLAND, which turns out to be very consistent with the ones from solar neutrino experiments. Since most non-standard effects in oscillations are dependent on the matter density (such as MVNs with acceleron couplings to matter fields, or non-standard flavor-changing matter effects generated by higher-dimensional operators), it is plausible to assume that strong constraints hold for the solar sector because of the very different environments/densities within the Sun and the Earth.

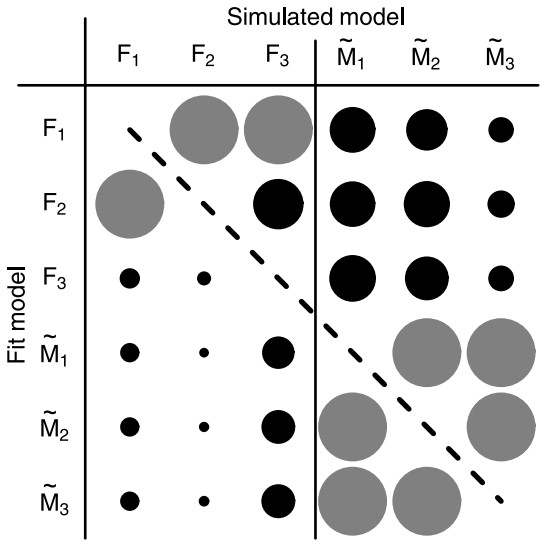

Fig. 3. Correlation between simulated models (*columns*) and fit models (*rows*). The areas of the disks represent the discovery potentials of the simulated "pure" effects (parameterized in terms of f_i or μ_i) given that a different pure effect (fit model) is allowed (minimum value of a deviation from zero necessary in either direction for a 3σ discovery). Therefore, the larger the disk, the more difficult it will be to distinguish a pure effect from another one. Note that we use cutoffs of $|f_i| \lesssim 0.3$ and $|\mu_i| \lesssim 0.5$ (*largest gray disks*), since some models cannot even be distinguished for much larger values. The areas of the rest of the disks are normalized with respect to these cutoffs for simulated flavor and mass effects

5.2 Identifying specific pure effects

If we discover a non-standard effect, it will be an interesting question how easily it can be identified. Assuming one dominating effect of the mass or flavor type, which we have introduced as "pure effect", we want to know how well it can be distinguished from other such effects of a different qualitative nature. Therefore, in Fig. 3, we show the correlation between simulated and fit pure effects. For this figure, we simulate a pure effect (column) and fit it with a different one (row), i.e., we marginalize over the respective f_i or μ_i. The areas of the disks are proportional to the minimum simulated value necessary to establish a 3σ effect, where we have chosen a cutoff of $|f_i| \lesssim 0.3$ and $|\mu_i| \lesssim 0.5$ (corresponding to the largest gray disks).[8] This means that the size of the disks measures the correlation between two pure effects and the ability to discriminate those.

One can easily make a number of qualitative observations from Sect. 3.2 quantitative. First, it is hard to discriminate between F_1 and F_2 (CP conserving and CP violating flavor-changing effects), since these effects are qualitatively similar and highly correlated with θ_{13} (as we have tested). However, if Nature implemented a flavor-changing F_1 or F_2 effect, then one could easily establish it against F_3 and the pure mass effects. In general, note that a discrimination between flavor and mass effects is rather easy because of their different spectral dependence in this example (such as between F_2 and $\tilde{M}_2$). The difference to F_3 can be explained by the different flavor-conserving nature of F_3. The results look somewhat different for the F_3-column: because of the correlation with ρ and all of the neutrino oscillation parameters (see below), it will be hard to establish this effect. For the simulated mass effects, the scale is

[8] Note that, for instance, the gray disks for f_1 and f_2 correspond to the order of magnitude of the upper bounds in (30), which means that testing considerably larger effects does not make sense.

different, i.e., one cannot directly compare the $\tilde{M}$-columns with the F-columns. Again, the mass effects can be distinguished from the pure flavor effects to some extent. However, it is quite impossible to establish a mass effect against another one, since they can easily be simulated by a different set of mass squared differences and mixing parameters with the same energy dependence. The only reason why the pure mass effects can be established in this example at all is that we have imposed external constraints on the solar parameters as motivated above.

5.3 Discovery of non-standard physics and potential for improvements

A very important issue of any pure non-standard effect is its evidence compared to the standard three-flavor oscillation scenario. Therefore, in Table 1, we show the discovery reaches for the parameters from (32) against the standard three-flavor neutrino oscillation scenario. This means that the pure effects shown are simulated and the standard three-flavor neutrino oscillation parameters are marginalized over. Comparing the precisions of f_1 and f_2 with the numbers in (30) is impressive. However, these discovery reaches depend on $\sin^2(2\theta_{13})$ (and $\delta_{\rm CP}$) and we have assumed a very large $\sin^2(2\theta_{13}) = 0.1$ (and $\delta_{\rm CP} = 0$). Note that the reach in f_2 is actually better than the one in f_1, which is different from what is found in the two-flavor limit in Sect. 3.2. The reasons are the mixing effects in the 2–3-sector and the fact that F_2 is a non-trivial source of CP violation in the three-flavor case.

Except from these sensitivities, which somewhat depend on the specific model, the behavior for neutrinos and antineutrinos, and so on, it may be of some interest to obtain hints on how these reaches can be improved. In order to study this aspect, we show the so-called "impact factors" for the test of specific simulated models against standard three-flavor neutrino oscillations in Fig. 4. These impact factors test the relative impact of the measurement errors on the neutrino oscillation parameters and systematics. In order to compute them, the non-standard discovery limits are evaluated with all neutrino oscillation parameters marginalized over, matter density uncertainties included, and systematics switched on (standard). In add-

Table 1. Discovery limits for the parameters in (32) as parameterized $f_i = F_i/V$ and $\mu_i = \tilde{M}_i/\Delta m^2_{31}$ from the neutrino factory simulation (including correlations)

Quantity	Lower limit (1σ)	Upper limit (1σ)	Lower limit (3σ)	Upper limit (3σ)
f_1	-0.008	0.008	-0.025	0.026
f_2	-0.003	0.003	-0.008	0.008
f_3	-0.016	0.016	-0.049	0.082
μ_1	-0.176	0.118	-0.218	0.211
μ_2	-0.105	0.126	-0.181	0.212
μ_3	-0.015	0.015	-0.044	0.090

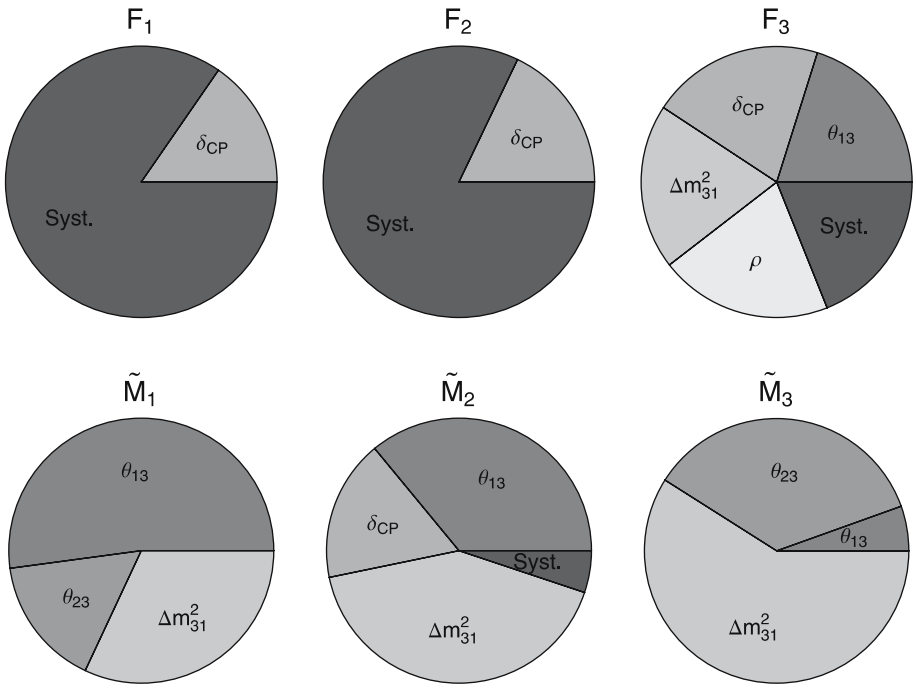

Fig. 4. Main impact factors (impact greater than 5%) for the test of specific simulated models (captions) against standard three-flavor neutrino oscillations (3σ measurement). The neutrino oscillation parameters refer to correlations with the respective parameter, "Syst." refers to systematics, and "ρ" refers to the matter density uncertainty. The impact factors are defined as in [57] as relative improvement when the respective quantity is fixed (correlations) or systematics is switched off

ition, in order to test a specific impact factor, one neutrino oscillation parameter is fixed at one time (or systematics is switched off), and the corresponding discovery reach for the non-standard effect is compared to the discovery reach including all uncertainties and systematics. The difference between these two discovery reaches describes the impact of a particular measurement error (or systematics), and the relative impact in Fig. 5 quantifies what one needs to optimize for in order to improve the discovery reach. For example, for $\tilde{M}_3$ (lower right pie), the error on Δm^2_{31} is the main impact factor in our model, which needs to be improved to increase the $\tilde{M}_3$ discovery reach.

Again, a number of aspects from Sect. 3.2 can be verified. For F_1 and F_2 effects, systematics is the main impact factor, since these flavor effects determine the overall height of the appearance signal and are not introduced with a specific spectral dependence (remember that we use a conservative overall normalization error of 2.5%). For F_3 effects, we have earlier determined the matter density uncertainty as an important constraint. However, improving the knowledge on Δm^2_{31}, θ_{13}, or $\delta_{\rm CP}$ does have a similar effect, since the extraction of the individual parameters becomes easier. For the mass effects, we encounter a completely different behavior. Remember that we have defined the mass effects with the same energy dependence as the mass squared differences, which means that particularly $\tilde{M}_3$ is easily mixed up with Δm^2_{31}. On the other hand, $\tilde{M}_1$ and $\tilde{M}_2$ are related to a flavor change in the appearance channel via the mixing matrix, i.e., the leptonic mixing angle θ_{13}. Therefore, it is not surprising that such a flavor change can be interpreted as either a mixing or a mass-changing effect. Compared to Sect. 3.2, there are also a number of differences coming from the three-flavor treatment (solar and CP effects) and the mixing in the 2–3-sector. These effects introduce additional correlations with θ_{23} and $\delta_{\rm CP}$. However, these are also the reason why, for example, $\tilde{M}_3$ can be constrained at all from this experiment alone [in the pure two-flavor case or without external constraints on the solar parameters, it would be impossible to distinguish between a non-vanishing $\tilde{M}_3$ and a different Δm^2_{31} if the mass effects had the energy dependence assumed in (32)].

5.4 Comparison to damping effects

In the context of the non-standard effect identification, a more general question is the ability to distinguish Hamiltonian effects and effects on probability level. The probability level effects lead to damping of the neutrino oscillation probabilities ("damping effects") and were studied in detail in [1]. They may originate from decoherence, neutrino decay, or other physics mechanisms. In this section, we address this identification in somewhat more detail in a qualitative manner. A relatively new ingredient for this identification is the use of the "silver" ($\nu_e \to \nu_\tau$) channel at a neutrino factory [74, 75]. It has been noticed [28, 65, 66] that the silver channel probability can be greatly enhanced for non-standard Hamiltonian effects. This corresponds to what we have found in Sect. 3.2, i.e., the silver channel, which is similar to the "golden" ($\nu_e \to \nu_\mu$) channel when there are no non-standard effects, behaves as our two-flavor limit in Sect. 3.2 for large energies.

In Fig. 5, we show the impact of different types of effects on the neutrino oscillation probabilities in the golden channel $P_{e\mu}$, the disappearance channel $P_{\mu\mu}$,[9] and the silver channel $P_{e\tau}$ (shown in columns) at a possible future neutrino factory (relevant energy range shown). The different rows correspond to scenarios with F_1 (flavor-changing without CP violation, Hamiltonian level), F_3 (flavor-conserving, Hamiltonian level), decoherence, and neutrino decay, respectively. The different model parameters for the different curves are given in the individual plots, where the thick curves correspond to the standard neutrino oscillation scenario. For a description of the decoherence and decay models, see [1]. In short, the decoherence model corresponds to standard wave packet decoherence, whereas the decay model assumes equal decay rates for all mass eigenstates (which can, for instance, be motivated by a degenerate mass spectrum). Note that this figure is shown for neutrinos only and that the comparison between the neutrino and antineutrino behavior can provide information on the underlying physics as well. However, this behavior is model dependent.

Figure 5 is very useful to study the characteristics of the different effects and to illustrate how the information from different neutrino oscillation channels can be used to disentangle them. First, it is important to note that it is difficult to construct a damping effect without large impact on the disappearance channel. Since the event rates in this channel are very high, it is probably the first place to look for non-standard physics. In addition, damping effects tend to suppress the golden and silver channel probabilities around the oscillation peak, which can, depending on the model, be very different for Hamiltonian level effects. However, as it can be read off from Fig. 5, Hamiltonian level effects produce, similar to $\sin^2(2\theta_{13})$, the largest effect in the appearance channels.[10] In particular, the flavor-conserving effect F_1 may enhance the silver probability as demonstrated in the two-flavor limit in Sect. 3.2. Comparing all panels in Fig. 5, we expect that the combination of all channels serves as a good model discriminator because each of the shown models has a unique signature if all these channels are combined. For example, we have tested that adding a 5 kt OPERA-like emulsion cloud chamber for the silver channel at the same baseline as the golden channel improves the F_1 discovery reach by about 60% (for simulation details, see [76]) because of the silver channel signature at large energies. There-

[9] The probability $P_{\mu\mu}$ is actually the ν_μ survival probability. However, this is the relevant probability when searching for the ν_μ disappearance rather than the disappearance probability $1 - P_{\mu\mu}$.

[10] The weak influence of the non-standard Hamiltonian level effects on the disappearance probability $1 - P_{\mu\mu}$ is purely due to the fact that (32) has been assumed for the non-standard Hamiltonian, where we have assumed the ν_μ states to be unaffected. However, as mentioned earlier, there are also stronger bounds on any NSI involving ν_μ.

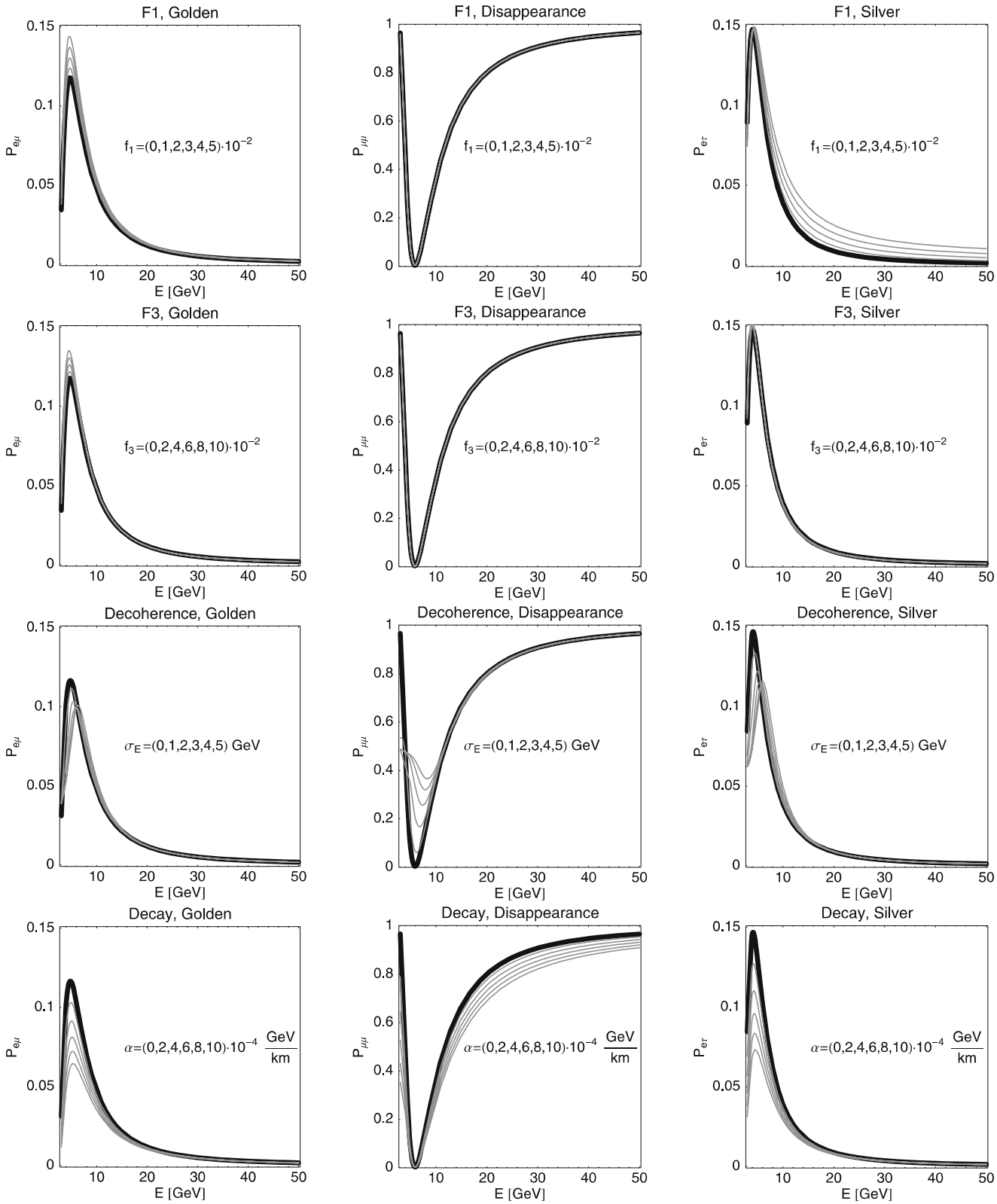

Fig. 5. The impact of four different non-standard effects (in rows) on three different oscillation channels (in *columns*): golden $\nu_e \to \nu_\mu$, disappearance $\nu_\mu \to \nu_\mu$, and silver $\nu_e \to \nu_\tau$. The different *rows* correspond to F_1 (flavor-changing without CP violation, Hamiltonian-level), F_3 (flavor-conserving, Hamiltonian-level), decoherence, and neutrino decay. The different model parameters for the different *curves* are given in the individual plots, where the *thick curves* correspond to the standard neutrino oscillation scenario

fore, we believe that this combination of different channels in combination with precise oscillation parameter measurements and spectral signatures can reveal non-standard physics.

6 Summary and conclusions

For future long-baseline neutrino oscillation precision measurements, such as neutrino factories, it will be an important question how to identify a non-standard effect. While it is very likely that many theoretical models will fit such a "new physics" discovery, the classification of models corresponding to this discovery from a phenomenological point of view will be very important for the planning of the following generation of experiments. Hence, there is strong interest in a top–down approach to non-standard physics tests, since the impact of future measurements on theory has to be assessed to promote the experiment. So far, mainly the bottom–up approach has been used, which is testing specific models in an experiment. Therefore, it has been one of the main goals of this work to demonstrate the identification and separation of individual phenomenological classes by generic arguments.

In summary, we have studied non-standard effects on neutrino oscillations on the Hamiltonian level. We have parameterized these effects in terms of the generators of the Lie algebra, and we have introduced them in flavor (such as coming from FCNC or NSI) and mass (such as coming from MVN) bases. As a trivial fact, there is, in principle, no mathematical difference between these effects if one allows for the most general form in each basis. Given the detection of a general non-standard effect on Hamiltonian level, it is therefore not possible to classify it as a flavor or mass effect without further assumptions or knowledge and, from an empirical point of view, the classification is a matter of definition. Therefore, we have defined "pure" effects as effects which are proportional to specific individual generators. Those correspond to pure flavor/mass conserving/violating effects, i.e., effects which affect particular flavor or mass eigenstates. This definition makes sense if one assumes that the underlying theoretical model causes one dominating non-standard effect. It is then the simplicity of the form in the respective basis which defines the effect to be of flavor or mass type. Therefore, the concept of these pure effects allows for the choice of the most "natural" class of models for further testing, which is most appealing from the physics point of view.

From the analytical point of view, we have studied the effects in the two-flavor limit. We have derived the modified mass squared differences and mixing angles (parameter mappings) as well as the modified resonance conditions including standard matter effects. In addition, we have discussed the application of this two-flavor limit to experiments, in particular, to the neutrino oscillation probability $P_{e\mu}$. This probability can be described to a first approximation by a two-flavor limit for large $\sin^2(2\theta_{13})$, where the $\sin^2(2\theta_{13})$ term dominates the CP effects. In addition, non-standard effects in the 1–3-sector have so far very poor limits (such as $\epsilon_{e\tau}$) and the driving parameter $\sin^2(2\theta_{13})$ is unknown, which means that there is room for confusion between θ_{13} and non-standard effects (see, e.g., [26, 27]). We have found that there are several generic features for different types of effects. While any flavor-violating pure effect can obviously change the transition probabilities, it does not affect the resonance condition/energy. However, a flavor-conserving pure effect changes the resonance condition similar to matter effects and is highly correlated with the matter density. In addition, it can suppress the flavor transition for large energies similar to matter effects – even in vacuum. Pure mass effects behave, in principle, as rotations of the flavor effects by the mixing angles, i.e., a pure mass effect will be observed as a linear combination of flavor effects. However, for a pure mass conserving effect, these flavor effects combine with special characteristics, since the mass effect is similar to an (energy dependent) change of the vacuum mass squared difference, i.e., it basically squeezes or stretches the oscillation pattern. Since in quantum field theory any non-standard effect may originate in the coherent (Hamiltonian effect) or incoherent ("damping" effect) summation of amplitudes, we have compared the non-standard Hamiltonian effects to the previously studied "damping" effects on probability level. We have found that these two classes can be distinguished by typical characteristics. Non-standard Hamiltonian effects shift the oscillation pattern, while "damping" effects, in general, do not. In principle, the different classes of non-standard Hamiltonian effects can be identified by their modification of oscillation amplitudes for large energies, the shift of the matter resonance, the comparison of different L/E-ranges, etc.

We have also studied some aspects of the three-flavor generalization of general non-standard Hamiltonian effects using perturbation theory as well as numeric calculations. By assuming small non-standard Hamiltonian effects, we have derived expressions for the effective matrix elements using perturbation theory and observed how the confusion theorem between θ_{13} and non-standard effects described in [27] arises at the Hamiltonian level. Our numeric calculations show that non-standard effects can alter the determination of θ_{13} significantly at higher energies, while still preserving a high accuracy at lower energies (cf. Fig. 2).

Eventually, we have demonstrated, by a numerical example for a neutrino factory, that many of these features can be found in a realistic experimental simulation using three flavors and specific spectral (energy) dependencies for the non-standard effects. For example, while it is simple to distinguish a flavor-changing effect from flavor-conserving or mass effects in general, mass effects are hard to establish as long as the neutrino oscillation parameters are not known from an independent source (such as with a different matter density for MVN). In addition, we have compared the obtainable discovery reaches for $\epsilon_{e\tau}$ to the current limits, and we have found at least an order of magnitude improvement for large $\sin^2(2\theta_{13})$ and $\delta_{\rm CP} = 0$. We have also compared the Hamiltonian level effects to damping effects and found that they can be distinguished by their specific al-

teration of the spectra in different neutrino oscillation channels.

Since the past has told us that neutrinos are good for surprises, the high-precision measurements at future neutrino oscillation experiments might as well reveal a detection of "new physics" beyond the standard model (extended to include massive neutrinos). Therefore, we conclude that one should include general strategies to look for non-standard effects in future neutrino oscillation experiments, where we have followed a top–down approach: instead of testing particular models (bottom–up), we have assumed that some inconsistency will be found first. Secondly, one may want to classify this inconsistency to be either a Hamiltonian or a probability level ("damping") effect. Finally, individual models are identified which fit this effect. Since we do not know exactly what we are looking for, such an approach might be a clever search strategy, and it can be useful to promote an experiment as a discriminator among different classes of theoretical models. Future studies should demonstrate how such an approach can be most efficiently extended to three neutrino flavors, which neutrino oscillation channels are most suitable, and what the correlations with the existing fundamental neutrino oscillation parameters imply.

Acknowledgements. W.W. would like to thank the Theoretical Elementary Particle Physics group at KTH for the warm hospitality during a research visit. In addition, T.O. and W.W. would like to thank Manfred Lindner and his group at TUM in Munich for the warm hospitality during their research visits where parts of this paper were developed.

This work was supported by the Royal Swedish Academy of Sciences (KVA), the Swedish Research Council (Vetenskapsrådet), Contract Nos. 621-2001-1611, 621-2002-3577, 621-2005-3588, the Göran Gustafsson Foundation, the Magnus Bergvall Foundation, the W.M. Keck Foundation, and NSF grant PHY-0070928.

Appendix A: General formalism for the two-flavor scenario

Any two-flavor Hamiltonian can be written in the flavor basis in the form

$$H = \mathbf{H}\cdot\sigma\,, \tag{A.1}$$

where $\mathbf{H}\in\mathbb{R}^3$ and $\sigma=(\sigma_1,\sigma_2,\sigma_3)$ is the vector of the three Pauli matrices (cf. the pictorial description of two-flavor neutrino oscillations in [77]). For a time-independent Hamiltonian, the time evolution operator is given by

$$S(t) = \exp(-\mathrm{i}Ht)\,. \tag{A.2}$$

Using the relation $(\mathbf{A}\cdot\sigma)^2=|\mathbf{A}|^2$, one obtains

$$S(t) = \mathbf{1}_2\cos(|\mathbf{H}|t) - \mathrm{i}\frac{H}{|\mathbf{H}|}\sin(|\mathbf{H}|t)\,, \tag{A.3}$$

where $\mathbf{1}_2$ is the 2×2 unit matrix. This gives the two-flavor neutrino oscillation probabilities of the form

$$P_{\alpha\alpha} = \mathrm{tr}[P_+S(t)] = 1-\sin^2(2\tilde\theta)\sin^2(kt)\,, \tag{A.4}$$

$$P_{\alpha\beta} = \mathrm{tr}[P_-S(t)] = \sin^2(2\tilde\theta)\sin^2(kt)\,, \tag{A.5}$$

where

$$P_\pm = \frac{1\pm\sigma_3}{2}\,,\quad \sin^2(2\tilde\theta) = \frac{H_1^2+H_2^2}{|\mathbf{H}|^2}\,,$$

$$k = |\mathbf{H}| = \sqrt{\sum_{i=1}^{3}H_i^2}\,.$$

Here the H_i are the components of the Hamiltonian and $\tilde\theta$ is the effective mixing angle.

In the standard two-flavor neutrino oscillation scenario, $H_1=\sin(2\theta)\Delta m^2/(4E)$, $H_2=0$, and $H_3=V/2-\cos(2\theta)\Delta m^2/(4E)$. In general, the resonance condition, i.e., the condition for maximal effective mixing, is $H_3=0$. The Hamiltonian is represented as a vector in $\mathbb{R}^3$, the third direction being the "flavor" eigendirection. The mixing is given by the angle between the Hamiltonian vector and the flavor eigendirection. The mixing is maximal, i.e., $\sin^2(2\tilde\theta)=1$, when the Hamiltonian vector is orthogonal to the flavor eigendirection, which, as expected, is equivalent to the resonance condition.

The flavor and mass bases, and thus, the flavor and mass effects, are intimately associated with each other. For the case of $n=2$, i.e., for two neutrino flavors, any effective contribution to the Hamiltonian can be written in either the flavor or mass basis, i.e., as $H'=F_1\rho_1+F_2\rho_2+F_3\rho_3$ or $H'=M_1\tau_1+M_2\tau_2+M_3\tau_3$. Since the effect must be the same regardless of the basis it is expressed in, we obtain the relations

$$\begin{cases} F_1 = M_1\cos(2\theta) - M_3\sin(2\theta)\,, \\ F_2 = M_2 \\ F_3 = M_1\sin(2\theta) + M_3\cos(2\theta) \end{cases} \tag{A.6}$$

from (7), i.e., one obtains F_1 and F_3 by rotating M_1 and M_3 by the angle -2θ and also one has $F_2=M_2$. Thus, the transformation in (A.6) relates flavor and mass effects and shows that they are linear combinations of each other.

Appendix B: Non-standard effects for large mixing

In this appendix, we concentrate on pure effects in the limit of large mixing. When the mixing goes to maximal, we have $\cos(2\theta)\to0$. This means that the resonance condition in (12) cannot be fulfilled for $F_3=0$ (i.e., "matter resonance") at reasonably large energies.[11] From (10), we can

[11] Note that, in this appendix, we assume that matter effects determine the resonance energy and the non-standard effects are sub-leading contributions, which may shift the resonance energy. Thus, we refer to the "matter resonance" as the resonance condition in (12) for $F_3=0$.

easily observe that F_1 and F_2 will not modify $\sin^2(2\tilde{\theta})$ at all in the absence of matter (and F_3) effects (for example, in $P_{\mu\mu}$ or a vacuum probability). Independent of matter effects, F_3 can increase the suppression of $\sin^2(2\tilde{\theta})$ for large energies. If the resonance condition in (12) is fulfilled, then $\sin^2(2\tilde{\theta})$ will be independent of F_1 and F_2. However, in the presence of matter effects (such as for P_{ee} in the limit $\theta_{13} \to 0$), F_1 and F_2 can reduce the matter effect suppression of $\sin^2(2\tilde{\theta})$ for large energies (cf. Fig. 6), i.e., they can increase the effective mixing. Eventually, it is obvious from (9) and (11) that the oscillation frequency is always increased for positive $F_i/\Delta m^2$.

It can also be interesting (and quite illuminating) to study how different pure (flavor or mass) effects affect the effective neutrino mixing and oscillations. In Fig. 6, we plot the effective mixing resulting from "pure" flavor and mass effects. From this figure, some features become quite apparent, e.g., some generic features are the shift in the resonance energy for F_3, M_1, and M_3, the non-zero high-energy mixing for all effects but the flavor-conserving effect F_3, and the appearance of an antiresonance – where $\sin^2(2\tilde{\theta})$ goes to zero for some finite energy – for F_1, M_1, and M_3.

The shift in the resonance energy is simply due to the shift in the H_3-component of the total effective Hamiltonian in the flavor basis (as was mentioned earlier, the resonance condition is $H_3 = 0$). The fact that there is no shift of the resonance condition for F_1 and F_2 was also discussed earlier.

The reason why the effective high-energy mixing generally turns out to be non-zero is also quite easy to realize. At high energies, the effective matter potential, which is diagonal in flavor basis, dominates over the vacuum Hamiltonian. As a result, the effective mixing is usually zero at high energies. However, if there is a non-standard effect with a corresponding effective addition to the Hamiltonian which is non-diagonal and is either constant or increasing with energy, then the effective mixing at high energies will be fully determined by the ratio of the non-standard effect and the matter potential.

The antiresonance appears when $H_1 = H_2 = 0$ in the flavor basis. Since $H_2 = 0$ in the standard neutrino oscillation scenario, it is apparent that this antiresonance will occur for some value of F_1. In addition, since M_1 and M_3 are linear combinations of F_1 and F_3, the antiresonance will also appear for M_1 and M_3 effects, as can be seen from the plots in Fig. 6.

There are also some interesting features that are specific for different effects. First, for F_1 effects, we note that the resonance condition is unchanged and that the mixing is constant as a function of energy for $F_1/V = -\tan(2\theta)/2$ (the reason for this is that the sum of the non-standard Hamiltonian and the matter potential is proportional to the vacuum Hamiltonian). Then, for flavor-conserving F_3 effects, we note that these correspond to changes in the effective matter potential. For $F_3/V < -1/2$, we obtain an effective matter potential which is negative, resulting in the disappearance of the resonance. Next, for M_1 effects, the mixing is constant when $M_1/V = -\sin(2\theta)/2$, in analogy with the F_1 effects (again, the reason is that the sum of the non-standard Hamiltonian and the matter potential is proportional to the vacuum Hamiltonian). Also in analogy with the F_1 effects is that there is a value of $2VE/\Delta m^2$, where the mixing does not depend on the M_1/V ratio. However, in the case of M_1 effects, this is not the resonance mixing, but rather a mixing of $\sin^2(2\tilde{\theta}) = \cos^2(2\theta)$, which appears at $2VE/\Delta m^2 = 1/\cos(2\theta)$. Finally, for mass conserving M_3 effects, we note that the resonance disappears when $2\cos(2\theta)M_3/V < -1$.

The reason why the equivalent F_2 and M_2 effects are not included is that these effects always lead to an increase in the effective mixing angle for all energies, and thus, those plots do not show as many interesting features as the plots included. In addition, we note that if the non-standard ef-

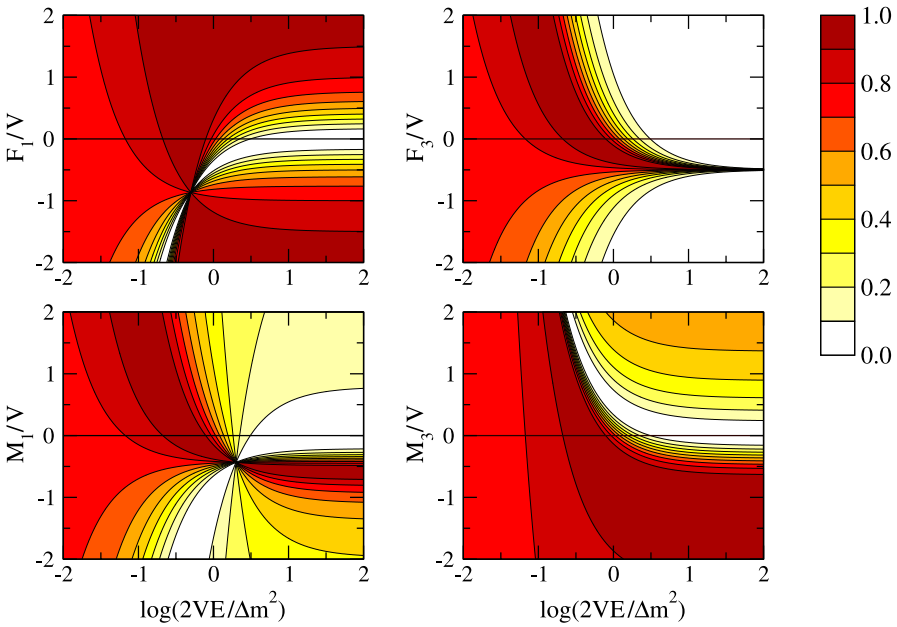

Fig. 6. The effective mixing $\sin^2(2\tilde{\theta})$ as a function of $2VE/\Delta m^2$ and the ratio between the pure flavor (F_1 and F_3) or mass (M_1 and M_3) effects and the matter potential V. The *horizontal lines* correspond to no non-standard effect and the mixing along them is therefore the same in all panels. The vacuum mixing is assumed to be $\theta = 30°$, which is close to the present value of the solar mixing angle θ_{12} (see, e.g., [62]). See the main text for a more detailed discussion

fects are energy dependent, then the effective mixing will be given by the mixing along some non-constant function of $2VE/\Delta m^2$ in Fig. 6.

Appendix C: Two-flavor limits of three-flavor scenarios

In this appendix, we discuss subtleties with the definition of the effective two-flavor scenarios introduced in Sect. 3.2. Remember that the effective two-flavor neutrino oscillation scenarios should be defined in terms of the effective two-flavor sector in question. For example, in the limit when $\Delta m^2_{21} \to 0$, the effective two-flavor sector is spanned by ν_e and $\nu_a = -s_{23}\nu_\mu + c_{23}\nu_\tau$. Thus, the limit can be considered as an exact pure two-flavor scenario only if the non-standard effects preserve the two-flavor limit (i.e., no off-diagonal terms mixing ν_e and ν_a with the remaining neutrino state $\nu_b = c_{23}\nu_\mu + s_{23}\nu_\tau$). If the non-standard addition to the Hamiltonian is given by

$$H'_{\alpha\beta} = \epsilon_{\alpha\beta} V \,, \tag{C.1}$$

then the corresponding addition in the basis spanned by $\{\nu_e, \nu_b, \nu_a\}$ is

$$H' = V \begin{pmatrix} \epsilon_{ee} & c_{23}\epsilon_{e\mu} - s_{23}\epsilon_{e\tau} & c_{23}\epsilon_{e\tau} + s_{23}\epsilon_{e\mu} \\ c_{23}\epsilon^*_{e\mu} - s_{23}\epsilon^*_{e\tau} & A & B \\ c_{23}\epsilon^*_{e\tau} + s_{23}\epsilon^*_{e\mu} & B^* & C \end{pmatrix}, \tag{C.2}$$

where

$$\begin{aligned} A &= c^2_{23}\epsilon_{\mu\mu} + s^2_{23}\epsilon_{\tau\tau} - s_{23}c_{23}(\epsilon_{\mu\tau} + \epsilon^*_{\mu\tau}) \,, \\ B &= c_{23}\epsilon_{\mu\tau} - s^2_{23}\epsilon^*_{\mu\tau} + s_{23}c_{23}(\epsilon_{\mu\mu} - \epsilon_{\tau\tau}) \,, \\ C &= s^2_{23}\epsilon_{\mu\mu} + c^2_{23}\epsilon_{\tau\tau} + s_{23}c_{23}(\epsilon_{\mu\tau} + \epsilon^*_{\mu\tau}) \,. \end{aligned}$$

From this relation, we deduce that the limit will be a pure two-flavor case if $\epsilon_{\alpha\beta} = 0$ for all non-standard effects which do not involve ν_e and $c_{23}\epsilon_{e\mu} - s_{23}\epsilon_{e\tau} = 0$ (which could be implemented by, e.g., $\theta_{23} = 45^\circ$ and $\epsilon_{e\mu} = \epsilon_{e\tau}$). In general, some of the conclusions for the two-flavor case will therefore not apply to three flavors. We have, in the numerical example in Sect. 5, demonstrated which of the conclusions do hold. The case when $\theta_{13} \to 0$ is similar to the case described above, with the exception that the effective two-flavor sector is now spanned by ν_e and ν_b instead of ν_e and ν_a. For the limit $\theta_{13} \to 0$ and $\Delta m^2_{32} \to 0$, there is no subtlety and the two-flavor sector is spanned by ν_μ and ν_τ.

References

1. M. Blennow, T. Ohlsson, W. Winter, JHEP **06**, 049 (2005) [hep-ph/0502147]
2. H. Päs, S. Pakvasa, T.J. Weiler, Phys. Rev. D **72**, 095 017 (2005) [hep-ph/0504096]
3. J.W.F. Valle, Phys. Lett. B **199**, 432 (1987)
4. J.W.F. Valle, J. Phys. G **29**, 1819 (2003) and references therein
5. S. Bergmann, Nucl. Phys. B **515**, 363 (1998) [hep-ph/9707398]
6. S. Bergmann, A. Kagan, Nucl. Phys. B **538**, 368 (1999) [hep-ph/9803305]
7. S. Bergmann, Y. Grossman, E. Nardi, Phys. Rev. D **60**, 093 008 (1999) [hep-ph/9903517]
8. L. Wolfenstein, Phys. Rev. D **17**, 2369 (1978)
9. P.I. Krastev, J.N. Bahcall, hep-ph/9703267
10. S. Bergmann, M.M. Guzzo, P.C. de Holanda, P.I. Krastev, H. Nunokawa, Phys. Rev. D **62**, 073 001 (2000) [hep-ph/0004049]
11. M. Guzzo et al., Nucl. Phys. B **629**, 479 (2002) [hep-ph/0112310]
12. A. Friedland, C. Lunardini, C. Peña-Garay, Phys. Lett. B **594**, 347 (2004) [hep-ph/0402266]
13. O.G. Miranda, M.A. Tórtola, J.W.F. Valle, hep-ph/0406280
14. S. Bergmann, Y. Grossman, D.M. Pierce, Phys. Rev. D **61**, 053 005 (2000) [hep-ph/9909390]
15. N. Fornengo, M. Maltoni, R.T. Bayo, J.W.F. Valle, Phys. Rev. D **65**, 013 010 (2002) [hep-ph/0108043]
16. M.C. Gonzalez-Garcia, M. Maltoni, Phys. Rev. D **70**, 033 010 (2004) [hep-ph/0404085]
17. A. Friedland, C. Lunardini, M. Maltoni, Phys. Rev. D **70**, 111 301 (2004) [hep-ph/0408264]
18. A. Friedland, C. Lunardini, hep-ph/0506143
19. G.L. Fogli, E. Lisi, A. Mirizzi, D. Montanino, Phys. Rev. D **66**, 013 009 (2002) [hep-ph/0202269]
20. B. Bekman, J. Gluza, J. Holeczek, J. Syska, M. Zrałek, Phys. Rev. D **66**, 093 004 (2002) [hep-ph/0207015]
21. S. Bergmann, Y. Grossman, Phys. Rev. D **59**, 093 005 (1999) [hep-ph/9809524]
22. T. Ota, J. Sato, Phys. Lett. B **545**, 367 (2002) [hep-ph/0202145]
23. T. Ota, J. Sato, N.-A. Yamashita, Phys. Rev. D **65**, 093 015 (2002) [hep-ph/0112329]
24. M.C. Gonzalez-Garcia, Y. Grossman, A. Gusso, Y. Nir, Phys. Rev. D **64**, 096 006 (2001) [hep-ph/0105159]
25. P. Huber, J.W.F. Valle, Phys. Lett. B **523**, 151 (2001) [hep-ph/0108193]
26. P. Huber, T. Schwetz, J.W.F. Valle, Phys. Rev. Lett. **88**, 101 804 (2002) [hep-ph/0111224]
27. P. Huber, T. Schwetz, J.W.F. Valle, Phys. Rev. D **66**, 013 006 (2002) [hep-ph/0202048]
28. M. Campanelli, A. Romanino, Phys. Rev. D **66**, 113 001 (2002) [hep-ph/0207350]
29. P. Gu, X. Wang, X. Zhang, Phys. Rev. D **68**, 087 301 (2003) [hep-ph/0307148]
30. R. Fardon, A.E. Nelson, N. Weiner, J. Cosmol. Astropart. Phys. **0410**, 005 (2004) [astro-ph/0309800]
31. V. Barger, P. Huber, D. Marfatia, hep-ph/0502196
32. M. Cirelli, M.C. Gonzalez-Garcia, C. Peña-Garay, Nucl. Phys. B **719**, 219 (2005) [hep-ph/0503028]
33. X.-J. Bi, P.-H. Gu, X.-L. Wang, X.-M. Zhang, Phys. Rev. D **69**, 113 007 (2004) [hep-ph/0311022]
34. P.Q. Hung, H. Päs, Mod. Phys. Lett. A **20**, 1209 (2005) [astro-ph/0311131]
35. D.B. Kaplan, A.E. Nelson, N. Weiner, Phys. Rev. Lett. **93**, 091 801 (2004) [hep-ph/0401099]
36. P.-H. Gu, X.-J. Bi, Phys. Rev. D **70**, 063 511 (2004) [hep-ph/0405092]

37. K.M. Zurek, JHEP **10**, 058 (2004) [hep-ph/0405141]
38. R.D. Peccei, Phys. Rev. D **71**, 023 527 (2005) [hep-ph/0411137]
39. H. Li, Z.-G. Dai, X.-M. Zhang, Phys. Rev. D **71**, 113 003 (2005) [hep-ph/0411228]
40. X.-J. Bi, B. Feng, H. Li, X.-M. Zhang, hep-ph/0412002 (2004)
41. R. Horvat, astro-ph/0505507
42. N. Afshordi, M. Zaldarriaga, K. Kohri, astro-ph/0506663
43. R. Takahashi, M. Tanimoto, hep-ph/0507142
44. R. Fardon, A.E. Nelson, N. Weiner, hep-ph/0507235
45. A.W. Brookfield, C. van de Bruck, D.F. Mota, D. Tocchini-Valentini, Phys. Rev. Lett. **96**, 061 301 (2006) [astro-ph/0503349]
46. M. Kawasaki, H. Murayama, T. Yanagida, Mod. Phys. Lett. A **7**, 563 (1992)
47. G.J. Stephenson Jr., T. Goldman, B.H.J. McKellar, Int. J. Mod. Phys. A **13**, 2765 (1998) [hep-ph/9603392]
48. G.J. Stephenson Jr., T. Goldman, B.H.J. McKellar, Mod. Phys. Lett. A **12**, 2391 (1997) [hep-ph/9610317]
49. R.F. Sawyer, Phys. Lett. B **448**, 174 (1999) [hep-ph/9809348]
50. S.P. Mikheyev, A.Y. Smirnov, Sov. J. Nucl. Phys. **42**, 913 (1985)
51. S.P. Mikheyev, A.Y. Smirnov, Nuovo Cim. C **9**, 17 (1986)
52. E.K. Akhmedov, R. Johansson, M. Lindner, T. Ohlsson, T. Schwetz, JHEP **04**, 078 (2004) [hep-ph/0402175]
53. T. Schwetz, W. Winter, Phys. Lett. B **633**, 557 (2006) [hep-ph/0511177]
54. J. Barranco, O.G. Miranda, C.A. Moura, J.W.F. Valle, hep-ph/0512195 (2005)
55. S. Davidson, C. Peña-Garay, N. Rius, A. Santamaria, JHEP **03**, 011 (2003) [hep-ph/0302093]
56. P. Huber, M. Lindner, W. Winter, Comput. Phys. Commun. **167**, 195 (2005) [hep-ph/0407333]
57. P. Huber, M. Lindner, W. Winter, Nucl. Phys. B **645**, 3 (2002) [hep-ph/0204352]
58. P. Huber, M. Lindner, M. Rolinec, W. Winter, Phys. Rev. D **73**, 053 002 (2006) [hep-ph/0506237]
59. G.L. Fogli, E. Lisi, A. Marrone, D. Montanino, Phys. Rev. D **67**, 093 006 (2003) [hep-ph/0303064]
60. J.N. Bahcall, M.C. Gonzalez-Garcia, C. Peña-Garay, JHEP **08**, 016 (2004) [hep-ph/0406294]
61. A. Bandyopadhyay, S. Choubey, S. Goswami, S.T. Petcov, D.P. Roy, hep-ph/0406328
62. M. Maltoni, T. Schwetz, M.A. Tórtola, J.W.F. Valle, New J. Phys. **6**, 122 (2004) [hep-ph/0405172]
63. R.J. Geller, T. Hara, Phys. Rev. Lett. **49**, 98 (2001) [hep-ph/0111342]
64. T. Ohlsson, W. Winter, Phys. Rev. D **68**, 073007 (2003) [hep-ph/0307178]
65. N. Kitazawa, H. Sugiyama, O. Yasuda, hep-ph/0606013
66. A. Friedland, C. Lunardini, Phys. Rev. D **74**, 033 012 (2006) [hep-ph/0606101]
67. CHOOZ Collaboration, M. Apollonio et al., Phys. Lett. B **466**, 415 (1999) [hep-ex/9907037]
68. H. Minakata, H. Nunokawa, JHEP **10**, 001 (2001) [hep-ph/0108085]
69. J. Burguet-Castell, M.B. Gavela, J.J. Gomez-Cadenas, P. Hernandez, O. Mena, Nucl. Phys. B **608**, 301 (2001) [hep-ph/0103258]
70. G.L. Fogli, E. Lisi, Phys. Rev. D **54**, 3667 (1996) [hep-ph/9604415]
71. A. Cervera et al., Nucl. Phys. B **579**, 17 (2000) [hep-ph/0002108]
72. M. Freund, P. Huber, M. Lindner, Nucl. Phys. B **585**, 105 (2000) [hep-ph/0004085]
73. M. Freund, Phys. Rev. D **64**, 053 003 (2001) [hep-ph/0103300]
74. A. Donini, D. Meloni, P. Migliozzi, Nucl. Phys. B **646**, 321 (2002) [hep-ph/0206034]
75. D. Autiero et al., Eur. Phys. J. C **33**, 243 (2004) [hep-ph/0305185]
76. P. Huber, M. Lindner, M. Rolinec, W. Winter, hep-ph/0606119
77. C.W. Kim, A. Pevsner, Contemporary Concepts in Physics, Vol. 8 (Chur, Switzerland: Harwood, 1993) p. 429